Available online at www.sciencedirect.com

ScienceDirect

Energy Procedia 00 (2008) 000–000

Energy Procedia

www.elsevier.com/locate/XXX

GHGT-9

CO_2 injection impairment due to halite precipitation

Nadja Muller[a]*, Ran Qi[b], Elizabeth Mackie[a], Karsten Pruess[c], Martin J. Blunt[b]

[a]*Shell International Exploration and Production B.V. , Kessler Park 1, Rijswijk 2288GS, Netherlands*
[b]*Department of Earth Science and Engineering, Imperial College, London SW7 2AZ, UK*
[c]*Lawrence Berkeley National Lab, 1 Cyclotron Road, Berkeley, CA 94720, US*

Elsevier use only: Received date here; revised date here; accepted date here

---

Abstract

The injection of dry supercritical CO_2 into brine aquifers has the potential to dry saline formation waters, due to evaporation effects [1], leading to severe increases in salinity and salt precipitation. This can significantly impair injection rates, as has been noted in gas-storage reservoirs.[2] This is of interest for CO_2 storage in saline aquifers. An injection impairment study was performed for the CO2SINK Project, a European Union research project on testing geological carbon storage near Ketzin, Germany [3]. Core flood experiments showed that halite precipitates due to brine evaporating in dry super-critical CO_2. The phenomenon was studied with two research codes, TOUGH2 and a streamline-based simulator. Both codes predict substantial salt deposition close to the injection point, with associated severe injection impairment. Our simulations also suggest that simple reservoir engineering measures, such as a brief (hours) preflush with fresh water, can mitigate adverse effects.

Keywords: CO_2 sequestration, salt precipitation, injection impairment

---

1. Introduction

Carbon storage in the subsurface is among the most promising immediately applicable climate change mitigation measures. However, dry supercritical carbon dioxide when injected into porous rock can evaporate saline water [1], leading to salt precipitation. This can significantly impair injection rates, as has been noted in gas-storage reservoirs.[2] The same problem is of interest for CO_2 storage in saline aquifers.

The behavior of the flow system is as follows. As dry CO_2 is being injected, the saline formation water is evaporated. Deep formation water can have solids in solution, with NaCl usually the most abundant. As the saline water is removed into the flowing CO_2 stream, the salt concentration increases and eventually reaches the solubility limit, giving rise to precipitation of salt. The precipitated solids reduce the pore space available to the fluids and may block the pore throats. The blocked pore throats do not permit fluid movement and hinder any further injection of carbon dioxide. The phenomenon occurs particularly in and close to the borehole, where large amounts of dry CO_2 move through the rock formation. This paper will present the combined results of supercritical CO_2 coreflood experiments and modelling sensitivities studies using the reservoir simulator TOUGH2/ECO2N [4, 5] and a

---

* Corresponding author. Tel.: +31-70-447-3379; fax: +31-70-447-5974.
E-mail address: Nadja.Muller@Shell.com.

streamline-based simulator [6]. The physical processes involved are complex and include cross flow of aqueous and CO_2-rich phases in the porous medium due to capillary effects, molecular diffusion of dissolved halite in the aqueous phase, and effects from increased density and viscosity of the aqueous phase at the evaporation front. Potential mitigation options have been investigated. A simple reservoir engineering solution can overcome severe halite precipitation close to the injection point by pre-flushing the formation with fresh water for a short period of time prior to CO_2 injection. Also altering the flow rate and pre-saturating CO_2 with water can prevent injectivity loss.

CO2SINK is a EU funded joint industry project. The German Research Centre for Geosciences is the project coordinator, in partnership with G.E.O.S. Freiberg, Geological Survey of Denmark and Greenland (GEUS), Mineral and Energy Economic Research Institute, Polish Acad. Sciences, DNV, Statoil, Shell, Institut für Wasserbau/ Universität Stuttgart, Vibrometric Cosma, University of Kent, Uppsala University, RWE Power, IEA Greenhouse Gas R&D Programme, Vattenfall Europe, Verbundnetz Gas, Siemens, E.ON Energie, and Schlumberger. The project aims to develop and demonstrate CO_2 storage techniques. The carbon dioxide is currently injected near the town of Ketzin, west of Berlin. One injection and two observation wells were drilled in 2007. Injection commenced on 30th June 2008. Up to August 24th 2008, 1740 tons of CO_2 were injected underground in an anticlinal structure of the Triassic Stuttgart formation [3]. The formation is a deltaic clastic sequence with quartz and feldspar as main mineral composites. The cross-bedded sand lies between 630 and 675 m underground. The thick Weser mudstone package overlies and seals the CO_2 storage sandstone. The injection interval was completed with screens between 632.2 and 654.2 m in the injector well. An interval of 15.49 m is open for injection. For more information go to website www.CO2Sink.org.

2. Methodology

This paper addresses only the Ketzin borehole injection area, not the full field. The evaporation phenomenon is not expected to occur throughout the reservoir, but only close to the injection point.

2.1. Model set-up

The salt precipitation due to CO_2 injection was modeled in several stages, from a very simple 1D radial model to a complex 3D model. In total, 60 000 tons of carbon dioxide are sequestered in the reservoir over 2 years.

Reservoir and injection conditions. The fluid and rock parameters are tabulated below in Table 1. Note that the carbon dioxide is injected in supercritical condition, though the reservoir is in sub critical CO_2 condition (pressure below critical point of ~ 73.1 bar).

Table 1 Ketzin storage - Stuttgart Formation. Fluid and rock properties for reservoir modelling.

Reservoir fluids properties		***Injection fluids properties***	
Reservoir temperature	35°C	Injection temperature	50°C
Reservoir pressure	63 bar	Max. injection pressure	82 bar
Reservoir fluid	NaCl-brine	Injection rate	1 kg/s
Brine density	1156 kg/m^3	Injection time	2 years
Brine salinity	22%	Injection fluid	100% dry CO_2
Reservoir rock properties			
Unit	Permeability range [mD]	Porosity [pu]	$P_0=\sqrt{\Phi/k}$
Weser mudstone	0.008 – 5.71	0.11 – 0.15	2.5 – 1.62
Stuttgart sandstone	41 – 234– 518	0.19 – 0.25 – 0.29	0.07 – 0.03- 0.02

Geometry. The numerical simulations use a relatively fine grid to achieve good spatial resolution and limit discretization errors.

1D radial model. In a zone surrounding the wellbore radius R_w = 0.2 m, up to R = 10 m where dry-out and precipitation are expected, we specify 100 grid blocks in logarithmic increments, starting from a first ΔR= 0.24m. The thickness is 16 m. The grid is extended to a large outer distance of 10,000 m, where boundary pressure conditions are maintained constant at initial values, to achieve an infinitely acting system.

3D model. The original geological model had X, Y, Z dimension of 5000 m x 5000 m x 150 m. Since halite precipitates close to the injection point, we needed only a near wellbore model. The original geological model had to be reduced in its lateral extension, but refined near the borehole ("down scaled"). This meant the permeability and porosity had to be refined. Referencing to the X, Y and Z coordinate of the injection well, the coordinate of each grid centre can be calculated based on the grid dimension. The "new" centre coordinate was mapped back to the original geological model to obtain the permeability and porosity value for this grid cell. The results of the permeability and porosity distribution in the refined near wellbore model are presented in Figure 1.

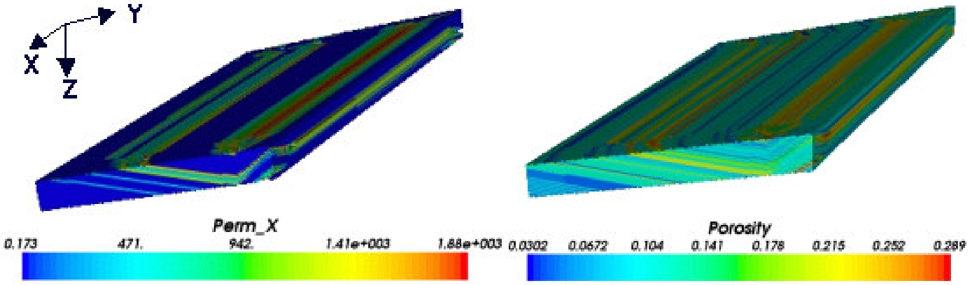

Figure 1: Horizontal permeability distribution (left) and porosity (right) of refined near wellbore model.

We took a 1000 m x 1000 m x 25 m subsystem near the wellbore region and refined the grid logarithmically in x – y direction. In a 30 m by 30 m region around the injection well are 100 by 100 grid cells with 0.3 m by 0.3 m grid size. From 30 m to 100 m are 10 by 10 grid cells with 7 m by 7 m grid size. From 100 m to 1000 m, the grid is the coarsest, with 30 m by 30 m and 30 by 30 grid cells in total. In the Z-direction, the perforation interval is 20 m. For concealment we added 2.5 m shale zones to the top and bottom of the system. Consequently, we have 25 layers with 1 m thickness in Z direction. The refined near wellbore model has in total 497,025 grid cells (141 x 141 x 25).

2.2. Permeability reduction model

When a solid precipitate occupies a fraction S_s ("solid saturation") of pore volume, the porosity available to the fluids is reduced from initial porosity Φ_0 to $\Phi = (1- S_s)*\Phi_0$. The corresponding reduction in permeability from k_0 to k depends on the geometric properties of the pore space, such as distribution of pore radii, pore bodies and throats, and connectivity. There is strong evidence from laboratory [7, 8] and field studies [9, 10] that modest reductions in porosity can cause severe reductions in permeability. In particular, in the studies cited above it was found that permeability may be reduced to zero at a finite porosity Φ_c, corresponding to a fraction $\phi_r = \Phi_c/\Phi_0$ of the original porosity. This behavior can be explained by a "tubes in series" model that considers pore space as consisting of a succession of pore bodies and throats, with pore bodies occupying a fraction of the path length. To predict the reduction in permeability caused by salt precipitation, we use the formulation of Verma and Pruess (1988) [11] for the "tubes in series" model. This model is coded in TOUGH2/ECO2N in the form $k/k_0 = f\left(\Phi/\Phi_0; \phi_r, \Gamma\right)$, where ϕ_r and Γ are adjustable parameters. The detailed expression for $f\left(\Phi/\Phi_0; \phi_r, \Gamma\right)$ can be found in reference [5]. The following form can approximate the tubes-in-series model with the relation for k/k_0.

$$\frac{k}{k_0} = \left(\frac{\Phi/\Phi_0 - \phi_r}{1-\phi_r}\right)^n$$

,which describes a power-law dependence of permeability on porosity, with k reduced to zero at a fraction ϕ_r of original porosity [10].

Experimental data (see below) were used to calibrate the permeability reduction in the TOUGH2 code, setting maximum modelled salt saturation (~16%) in relation to observed maximum permeability reduction (~60%). The parameters ϕ_r and Γ were assumed equal, resulting in $\phi_r = \Gamma = 0.567$.

2.3. Relative permeability function

CO_2 and water relative permeability relations have not been studied as extensively as oil-brine systems. Since no relative permeability data from the Ketzin reservoir rock were available at the time of this study, we used experimental data from literature. Bennion and Bachu (2006) [12] conducted core experiments on sandstones and carbonates to establish super-critical CO_2 and brine relative permeability. The closest match to the Ketzin reservoir is the Viking sandstone they studied with an absolute air permeability of 5.78 mD. However, the experimental parameters are not the same as the Ketzin reservoir properties, and were consequently only used to guide an approximation. The van Genuchten – Mualem model was used to fit the experimental data, see Figure 2. Note that the experimental data suggest a very high residual water saturation, which corresponds to a very low CO_2 relative permeability. The liquid relative permeability (brine) of the van Genuchten – Mualem model can be described as follows [13]:

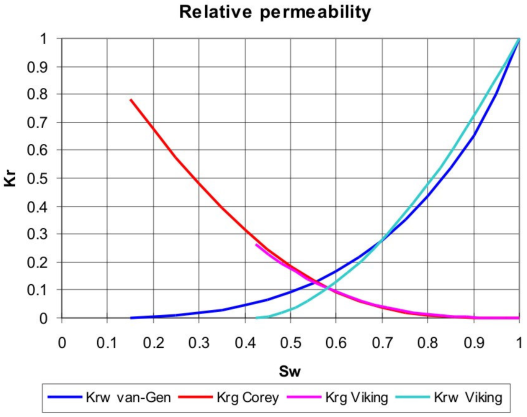

$$k_{rl} = \begin{cases} \sqrt{S^*}\left\{1-\left(1-[S^*]^{1/\lambda}\right)^{\lambda}\right\}^2 & \text{if } S_l < S_{ls} \\ 1 & \text{if } S_l \geq S_{ls} \end{cases}$$

Figure 2: Relative permeability function comparison of experiment with theoretical model.

where k_{rl} is the relative brine permeability, S_{ls} the maximum brine saturation, S_l the brine saturation, λ defines the curvature of the relative permeability curves and $S^* = (S_l - S_{lr})/(S_{ls} - S_{lr})$. S_{lr} is the connate water saturation. The Corey function was used to match the gas relative permeability (CO_2) [14].

In Figure 2, “Krg Corey” presents relative permeability CO_2 and “Krw van-Gen” the relative permeability of brine of the van Genuchten – Mualem model. “Krg Viking” and “Krw Viking” are the experimental relative permeabilities of CO_2 and brine. The following endpoints were input for the theoretical model: Slr = 0.05; Sls = 1; Sgr = 0.05; $\lambda = 0.85$. The resulting output endpoints are Krg = 0.78 @ connate water saturation = 0.15.

2.4. Capillary pressure function

The capillary pressure measurements of the Ketzin reservoir rock were not available at the time. Equally, no reliable literature data was available. A successful field-simulation match was achieved by Doughty et al. [15] for the Frio CO_2 injection test, using the van Genuchten capillary pressure function [16]. Since the petrophyscial parameters of the Frio reservoir rock and the Stuttgart sandstone are similar, we chose the same capillary pressure relationship: [13]

$$P_{cap} = -P_0\left([S^*]^{-1/\lambda} - 1\right)^{1-\lambda}$$

where P_{cap} is the capillary pressure, $S^* = (S_l - S_{lr})/(S_{ls} - S_{lr})$, λ defines the curvature of the capillary pressure function and P_0 the strength coefficient. Due to the lack of experimental data, P_0 was derived from the data of Doughty et al. [15] by applying the following Leverett scaling [17].

$$P_0 \cong \sqrt{\frac{\Phi}{k}}$$

Using the corrected core porosity and permeability of the Ketzin reservoir rock, the P_0 values were evaluated for each permeability-porosity unit in the TOUGH2 simulation. λ is 0.457.

2.5. Codes

TOUGH2 is a numerical simulator for nonisothermal flows of multicomponent, multiphase fluids in one, two, and three-dimensional porous and fractured media. The chief applications for which TOUGH2 is designed are in geothermal reservoir engineering, nuclear waste disposal, environmental assessment and remediation, and unsaturated and saturated zone hydrology. [13] ECO2N is a fluid property module for the TOUGH2 that was designed for applications to geologic sequestration of CO_2 in saline aquifers. [5]

We also used a three-dimensional streamline simulator, originally developed at Stanford University that has been modified to simulate CO_2 transport in aquifers and oil reservoirs. Streamline-based simulation is a method to model multiphase flow in heterogeneous media; fluid is transported along streamlines that follow the instantaneous total velocity. This accurately and efficiently tracks fluid movement, resulting in reduced numerical dispersion, grid orientation effects and run time compared to conventional grid-based methods. This technique is used in the petroleum industry for modelling flow dominated by reservoir heterogeneity. Streamlines are ideal for representing the complex flow paths in multidimensional models.

Code comparison functionalities	TOUGH2-ECO2N	IC-3DSL
Capillary pressure	✓	✗
Relative permeability	✓	✓
Molecular diffusion	✓	✓
Non-isothermal	✓	✓
Compressible flow	✓	✗
Heat exchange with impermeable layers	✓	✗
Mutual solubility CO_2-brine	✓	✓
Geomechanical effects	✗	✗
Streamline	✗	✓
CO_2 viscosity/density dynamic	✓	✗
Geochemical effects - reactive flow	Halite precipitation /dissolution only	Halite precipitation /dissolution only

Table 3: TOUGH2-ECO2N [5] and stream-line simulator [18] functionality comparison table

2.6. Coreflood experiments

A dry clean analogue Berea core (2.5 cm diameter, 28 cm long) with 100 mD and around 20 % porosity was saturated with 25% salinity NaCl brine and flushed with supercritical CO_2 for 32 hours at CO2SINK conditions (see Table 1). The steady state gas permeability was measured before and after the experiment.

3. Results

3.1. Experimental results

The observed CO_2 permeability was reduced by approx. 60% due to halite precipitation over the entire pore network of the Berea sandstone core.

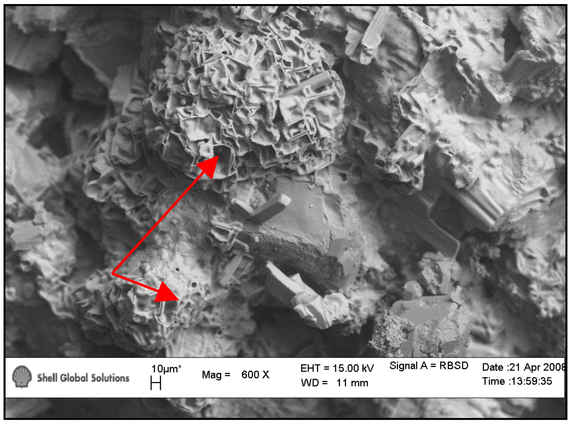

The SEM and ESEM images and elemental analysis confirm the presence of halite and show crystals precipitated throughout the flow direction of core in a variety of morphologies (platy and hopper crystals [19]). The precipitation appears to coat the quartz grains in rafts of platy crystals over the pore throats and grains. The smallest crystals are observed at the outlet of the core. Significantly, Hopper halite crystals (skeletal morphology i.e. hollow stepped crystals [19]) are also observed. Hopper crystals are indicative of rapid rates of crystallization due to a high degree of super saturation. The observed permeability was reduced to approx. 60% after 32 hrs of flooding. The models calculated that halite solids occupy up to ~16% of the available pore space.

Figure 3: ESEM photograph of Berea sandstone after 32hrs of CO_2 flooding. Red arrows point at Hopper NaCl crystals.

3.2. Modeling dry CO_2 injection with TOUGH2 – 1D simulation

Dry supercritical CO_2 is injected with 1 kg/s for 2 years. The injected CO_2 displaces brine (see Figure 4a) and a small fraction dissolves in the brine, while some of the saline formation water evaporates into the flowing CO_2 stream. Water uptake occurs only in the immediate vicinity of the injection point. With ongoing injection the liquid phase becomes enriched with salt because more saline water evaporates (Figure 4b). The liquid phase consists of water, dissolved salt in the form of halite (NaCl) and carbon dioxide. Figure 4b shows that the concentration of dissolved NaCl increases sharply before the onset of solid deposition. The solids are the salt precipitating from the brine (Figure 4c). The salt precipitation peaks at 16.6%, 0.3 m from the borehole. Once the injection is stopped, the brine re-invades the dried up zone (see curves 1 yr and 2 yrs after the end of injection in Figure 4c).

The halite precipitation leads to a pore geometry change. The absolute permeability is reduced to as little as 40% near the injection well (see Figure 4d), as calibrated by the lab experiments. Halite is deposited up to 5 m into the formation (Figure 4d). After the end of injection, the saline formation water returns to the evaporation region, dissolving salt (see brown curve “2yrs after inj.stop” in Figure 4d). The freed pore space is occupied by more brine and CO_2 two years after the end of injection (see in Figure 4a).

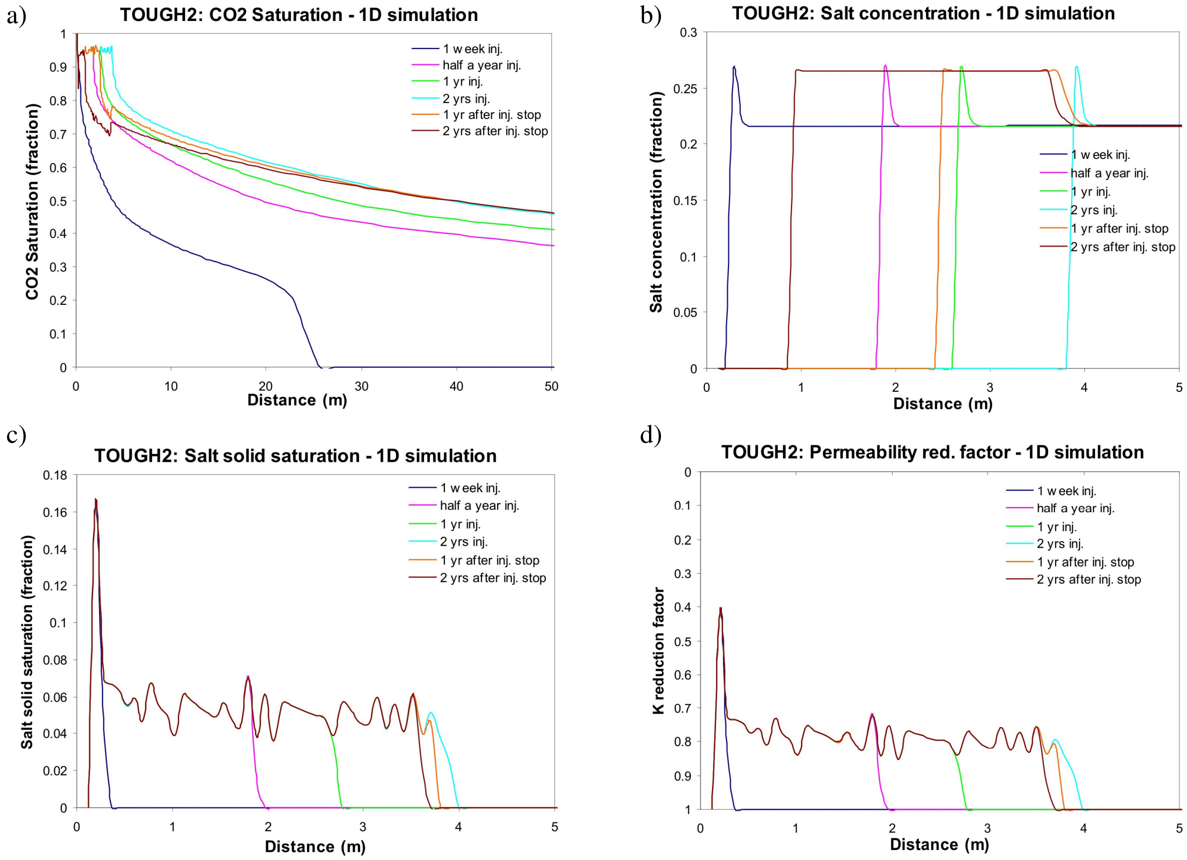

Figure 4: CO_2-NaCl-sytem during and after CO_2 injection, TOUGH2 results. The five figures show the evolution of the system over time and distance from the injection point at 0 m. Each curve presents a time snapshot at 1 week, half a year, one year and two years of injection. The CO_2 invasion is shown in Figure a). The salt concentration in the brine is given in Figure b). Salt precipitation occupies more pore space over injection time (Figure c), resulting in a permeability reduction (see Figure d), note the K reduction is given as factor of the absolute K).

3.3. Modeling dry CO_2 injection after water flood with TOUGH2 – 1D simulation

The Stuttgart formation was flushed with brackish water (8,000 ppm salt; T = 30°C) for 16.2 hours at a rate of 1kg/s (total amount 362bbl). After 1 week dry CO_2 injection started and was continued for 2 years. Figure 5 shows that no halite was deposited up to 1 m distance from the injection point. Salt solids formed in the pore space beyond, with a maximum 4% at 4.3 m.

The salt concentration increases in a gentle slope after one week of injection (blue line in Figure 5), contrary to the CO_2 injection without pre-flush (see Figure 4). This reflects the fresh water flood and how the salinity gradient was pushed away from the borehole. Salt concentration increases at further distance from the injection point with injection time. Sharp peaks indicate the onset of salt precipitation. Note that the maximum brine solubility limit of 26% is never reached during injection in the near wellbore region. Only when the brine re-invades the dried out region after the injection stop, do we observe maximum salt concentration (see orange and brown curve in Figure 5).

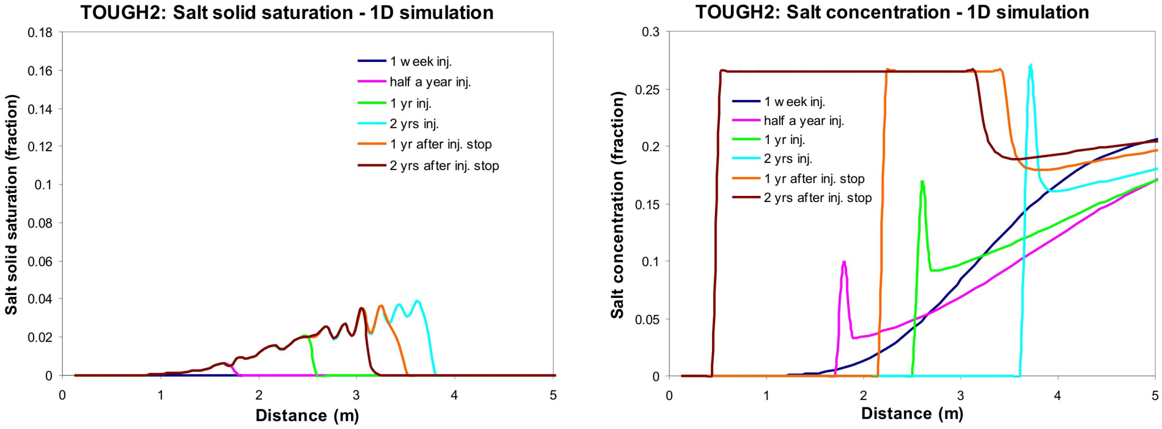

Figure 5: NaCl concentration in solution and salt solids over time and distance after water pre-flush and CO_2 injection. Results from TOUGH2.

3.4. Modeling dry CO_2 injection with a streamline simulator - 3D simulation

After one year of dry CO_2 injection, Figure 6 shows that salt solids occupy already in a relatively large area near the wellbore. With time the saturation becomes more distinct, until it reaches a horizontal extent of 18 m at the end of injection. It can be observed that CO_2 chooses the path of least resistance, which are the high permeability layers (compare Figure 1 and Figure 5). Due to the buoyant nature of CO_2, the salt precipitation phenomenon progresses towards the top of the reservoir. Note the high k layer on top of the reservoir with conspicuous halite precipitation. Overall, we observe that the reservoir heterogeneity enforces localized maxima of salt precipitation where large amounts of CO2 move through the rock.

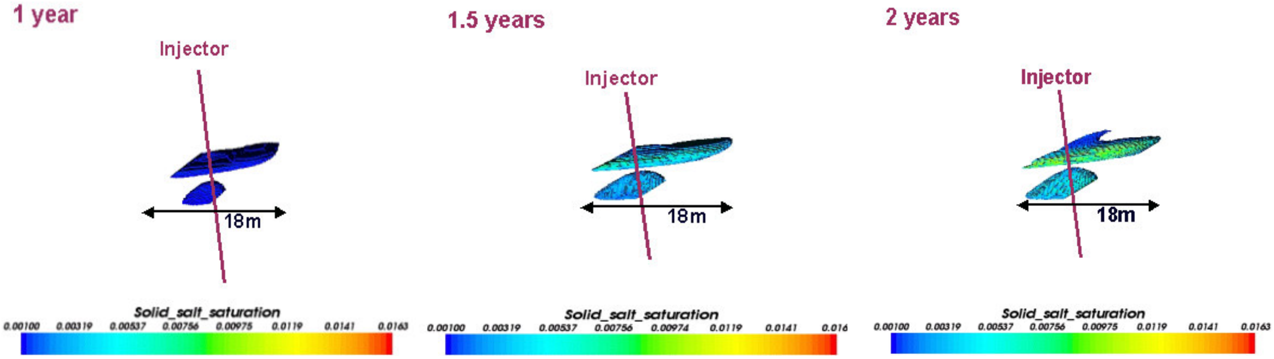

Figure 6: Solid salt saturation distribution after dry CO2 injection over time. 3D results from streamline simulator.

4. Conclusions

Core flood experiments with analogue Berea sandstone confirmed the presence of halite precipitation after flushing a NaCl saturated core with dry super-critical CO_2. The halite precipitation was studied with two research codes, TOUGH2 and a streamline-based simulator. Both codes predict rather substantial salt deposition close to the injection point under CO2SINK reservoir and injection conditions. The combined experimental and modeling work suggests that this phenomenon can severely reduce the injectivity of CO_2 in saline aquifers. However, there are simple reservoir engineering measures that can be taken to mitigate adverse precipitation effects. A brief (16.2 hours) fresh water pre-flush prior to CO2 injection was shown to prevent precipitation and pore blockage close to the borehole. Precipitation still occurs, but is less spatially concentrated and further out in the formation. Hence, the injection impairment can be mitigated. Another potential mitigation measure that should be explored is pre-saturating CO2 with water prior to injection. This is expected to avoid brine evaporation and salt precipitation. Also, sensitivity of precipitation behavior to parameters such as salinity, flow rate, absolute permeability and capillary pressure need to be studied in heterogeneous 2D and 3D models and in laboratory experiments.

Acknowledgment

The CO2SINK project received its funding from the European Commission, the Federal Ministry of Economics and Technology, the Federal Ministry of Education and Research and the industry partners (Shell, Statoil, RWE, Vattenfall, Schlumberger and VNG). For more information go to website www.CO2Sink.org.

Reference

1. Spycher, N., K. Pruess, and J. Ennis-King, *CO2-H2O mixtures in the geological sequestration of CO2. I. Assessment and calculation of mutual solubilities from 12 to 100°C and up to 600 bar.* Geochimica et Cosmochimica Acta, 2003. **67**(16): p. 3015-3031.
2. Kleinitz, W., M. Köheler, and G. Dietzsch. *The precipitation of salt in gas producing wells.* in *SPE European formation damage conference*. 2001. The Hague, The Netherlands: SPE.
3. Förster, A., et al., *Baseline characterization of the CO2SINK geological storage site at Ketzin, Germany* Environmental Geosciences, 2006. **13**(3): p. 145-161.
4. Pruess, K., *The TOUGH Codes--A Family of Simulation Tools for Multiphase Flow and Transport Processes in Permeable Media.* Vadose Zone J., 2004. **3**(3): p. 738-746.
5. Pruess, K., *ECO2N: A TOUGH2 fluid property module for mixtures of water, NaCl, and CO2.* 2005, Lawrence Berkeley National Laboratory: Berkeley, CA. p. 76.
6. Batycky, R.P., M.J. Blunt, and M.R. Thiele, *A 3D Field-Scale Streamline-Based Reservoir Simulator* SPE Reservoir Engineering, 1997. **12**(4): p. 246-254.
7. Morrow, C., et al., *Permeability of Granite in a Temperature Gradient.* Journal of Geophysical Research, 1981. **86**(84): p. 3002-3008.
8. Vaughan, P.J., *Analysis of Permeability Reduction During Flow of Heated, Aqueous Fluid Through Westerly Granite.* Coupled Processes Associated with Nuclear Waste Repositories, ed. C.F. Tsang. 1987, New York: Academic Press. 529 - 539.
9. Pape, H., C. Clauser, and J. Iffland, *Permeability Prediction Based on Fractal Pore-Space Geometry.* Geophysics, 1999. **64**(5): p. 1447 - 1460.
10. Xu, T., et al., *Reactive transport modeling of injection well scaling and acidizing at Tiwi field, Philippines.* Geothermics, 2004. **33**(4): p. 477-491.
11. Verma, A. and K. Pruess, *Thermohydrologic Conditions and Silica Redistribution Near High-Level Nuclear Wastes Emplaced in Saturated Geological Formations.* Journal of Geophysical Research, 1988. **93**(B2): p. 1159-1173.
12. Bennion, D.B. and S. Bachu. *Supercritical CO2 and H2S—Brine Drainage and Imbibition Relative Permeability Relationships for Intergranular Sandstone and Carbonate Formations* in *SPE Europec/EAGE Annual Conference and Exhibition*. 2006. Vienna, Austria.
13. Pruess, K., C. Oldenburg, and G. Moridis, *TOUGH2 user's guide, version 2.0.* 1999, Lawrence Berkeley National Laboratory: Berkeley. p. 210.
14. Corey, A.T., *The Interrelation Between Gas and Oil Relative Permeabilities.* Producers Monthly, 1954. **19**(1): p. 38-41.
15. Doughty, C., B. Freifeld, and R. Trautz, *Site characterization for CO2 geologic storage and vice versa: the Frio brine pilot, Texas, USA as a case study.* Environmental Geology, 2008. **54**(8): p. 1635-1656.
16. van Genuchten, M.T., *A Closed-form Equation for Predicting the Hydraulic Conductivity of Unsaturated Soils.* Soil Science Society of America Journal, 1980. **44**(5): p. 892-898.
17. Leverett, M.C., *Capillary Behavior in Porous Solids.* Trans. Soc. Pet. Eng. AIME, 1941. **142**: p. 152-169.
18. Qi, R., et al. *Design of Carbon Dioxide Storage in a North Sea Aquifer Using Streamline-Based Simulation.* in *SPE Annual Technical Conference and Exhibition*. 2007. Anaheim, CA, US.
19. Phillips, F.C., *An Introduction to Crystallography*. 2nd ed. 1956: London, Longmans, Greens & Co. 324.